CrystEngComm

Accepted Manuscript



This is an *Accepted Manuscript*, which has been through the RSC Publishing peer review process and has been accepted for publication.

Accepted Manuscripts are published online shortly after acceptance, which is prior to technical editing, formatting and proof reading. This free service from RSC Publishing allows authors to make their results available to the community, in citable form, before publication of the edited article. This Accepted Manuscript will be replaced by the edited and formatted Advance Article as soon as this is available.

To cite this manuscript please use its permanent Digital Object Identifier (DOI®), which is identical for all formats of publication.

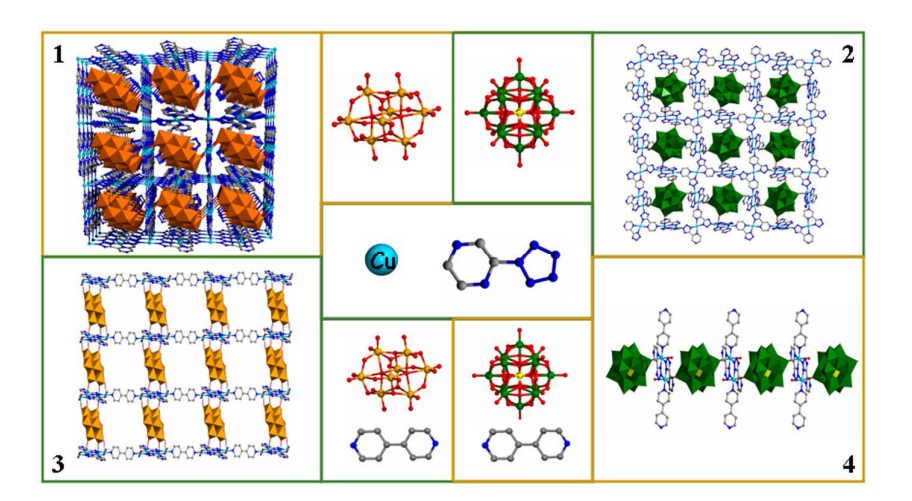
More information about *Accepted Manuscripts* can be found in the **Information for Authors**.

Please note that technical editing may introduce minor changes to the text and/or graphics contained in the manuscript submitted by the author(s) which may alter content, and that the standard **Terms & Conditions** and the **ethical guidelines** that apply to the journal are still applicable. In no event shall the RSC be held responsible for any errors or omissions in these *Accepted Manuscript* manuscripts or any consequences arising from the use of any information contained in them.

Tuning the Dimension of the POM-based Inorganic-organic Hybrids from 3D Self-penetrating Framework to 1D Poly-pendant Chain *via* Changing POM Clusters and Introducing Secondary Spacers†

Shaobin Li, Huiyuan Ma*, Haijun Pang*, Zhuanfang Zhang, Yan Yu, Heng Liu and Tingting Yu

The four compounds show distinct structure motifs from 3D self-penetrating framework to 1D poly-pendant chain, which illustrate that the POMs and the secondary spacers are key factors to tune the dimension of the POM-based hybrids. Additionally, the luminescent and electrochemical properties for compounds **1–4** have been investigated.



Tuning the Dimension of the POM-based Inorganic-organic Hybrids from 3D Self-penetrating Framework to 1D Poly-pendant Chain *via* Changing POM Clusters and Introducing Secondary Spacers†

Shaobin Li, Huiyuan Ma*, Haijun Pang*, Zhuanfang Zhang, Yan Yu, Heng Liu and Tingting Yu

Key Laboratory of Green Chemical Engineering and Technology of College of Heilongjiang Province, College of Chemical and Environmental Engineering, Harbin University of Science and Technology, Harbin 150040, China Tel.: 86-0451-86392716, Fax: 86-0451-86392716; E-mail: mahy017@163.com (Ma H. Y.), panghj116@163.com (Pang H. J.).

Abstract

Through tuning the different polyoxometalate (POM) clusters and the secondary spacers, four new various dimensionalities inorganic-organic hybrid compounds $Cu_5(pzta)_6(H_2O)_2[Mo_8O_{26}]$ (1), $Cu_5(pzta)_6(H_2O)_6[PW_{12}O_{40}]\cdot(OH)$ (2), $Cu_4(pzta)_2(bipy)(H_2O)_4(OH)_2[Mo_8O_{26}]\cdot 2H_2O$ (3) and $[Cu_2(pzta)_2(bipy)_2(H_2O)_2][HPW_{12}O_{40}]\cdot 8H_2O$ (4) (pzta = 5-(2-pyrazinyl) tetrazole, bipy = 4,4'-bipyridine have been synthesized under the identical hydrothermal conditions. The four compounds were assembled from copper cations, N-donor ligands and POM clusters. Compound 1 displays novel self-penetrating 3D framework. When the POM clusters were changed from β -[Mo₈O₂₆]⁴⁻ (β -Mo₈) to

[PW₁₂O₄₀]³⁻ (PW₁₂), compound **2** was obtained, and it is a 2D layer with square channels, into which the tetradentate PW₁₂ anions as templates are incorporated. Furthermore, by introducing second spacer bipy into the reaction system of **1** and **2**, respectively, compounds **3** and **4** were obtained. **3** shows a 2D layer that consists of the adjacent metal-organic chains fused together by six connected β-Mo₈ anions, and **4** exhibits a 1D poly-pendant chain constructed by dinuclear copper complexes and PW₁₂ clusters. The distinct structural features of the four compounds suggest that different POM clusters and the secondary spacers should have great effect on the structures of POM-based inorganic-organic hybrids. Additionally, the luminescent and electrochemical properties for **1–4** have been investigated.

Introduction

Inorganic-organic hybrids are a new generation of solid-state materials that have various structures as well as wide-ranging applications, such as in catalysis, gas storage and materials science^{1,2} Polyoxometalates (POMs) are the versatile inorganic building blocks and possess the superior potential applications in catalysis, electrochemistry and magnetism.³⁻⁵ In virtue of their special properties, it is appealing to constructed POM-based inorganic-organic hybrids. To date, thanks to the work of POM chemists,⁶ many novel POM-based inorganic-organic hybrids have been successfully synthesized. Nevertheless, in the crystal engineering point of view, the control of self-assembly processes is still a very challenging work to realize the targeting syntheses of the POM-based inorganic-organic hybrids, because the final

structures are frequently influenced by various factors, such as metal ions, ⁷ pH value, ⁸ and steric hindrance, length, and flexibility of organic ligands. ⁹

It is well-known that organic spacers play significant roles in the construction of inorganic-organic hybrids with novel structures and improved properties. ¹⁰ Compared with single ligands, mixed-ligands consist of two kinds of spacers and provide more variability to build much more fascinating structures. Recent trends for the controlled synthesis of inorganic-organic hybrids, is a use of a new mixed-ligand system which aim to control the resulting structure and lead to further diversification of the frameworks with fascinating structures. 11 The synthesis by using the mixed-ligand system has an advantage that can be controlled by means of the stepwise construction of the structure; first step introducing the primary spacer to form the initial framework and then at the second step, it can further modify the functionality by introducing the second spacer by self-directing reaction to realize the various dimensional architectures. However, in the POM-based inorganic-organic hybrids system, the influential principles of the mixed-ligands are less ascertained. 12 Those previously reported POM-based hybrids can be roughly divided to three types according to the mixed ligands (please see the table S1), type I, one organoamine and one dicarboxylate ligands, type II one linear/chelating and one chelating organoamine ligands and type III, one multidentate and one linear organoamine ligands. Among the three types of POM-based hybrids constructed by mixed-ligands, the type III is rarely obtained, and to the best of knowledge there are only three compounds have been reported in the very recently. 12i, j The multidentate rigid ligand 5-(2-pvrazinvl)

tetrazole (pzta) possesses flexible coordination modes (Scheme 1) due to their six potential N-coordination sites, namely the adjacently four N atoms of tetrazolyl and the two N atoms of pyrazinyl, and thus the pzta is readily available to coordinate metal ions for affording polynuclear metal clusters. And such polynuclear metal clusters have multiple coordination sites, which are in favor of forming high-dimensional hybrids. Furthermore, compared with neutral ligands, the pzta is deprotonated ligand from neutral Hpzta molecule possessing a negative charge and thus the pzta has a significant affinity to coordinate to more cations forming the complicated structures with ease. In addition, the linear rigid 4,4'-bipy organoamine molecule that contains two terminal pyridyl groups in the opposite positions is a candidate as the secondary spacer to tune the dimensionality of final compounds, which has been widely explored in constructing inorganic-organic hybrids. On the other hand, the POM polyanion is another key factor that can influence dimension of inorganic-organic hybrids.¹³ The POMs exhibit a wide variety of structural motifs with different sizes and shapes, ranging from closed cages and spherical shells to basket-, bowl-, barrel- and belt-shaped structures¹⁴. Therefore, when different POMs are used as modular inorganic building blocks, it is difficult to predict the topology of inorganic-organic hybrids. And it is desirable to study systematically the roles of POMs in the assembly of the inorganic-organic hybrids.

Scheme 1. View of the typical coordination modes of pzta ligand.

Herein, we study on a hydrothermal reaction system of copper, pzta/bipy mix-ligands and β-Mo₈/PW₁₂ POMs in detail, and four new compounds Cu₅(pzta)₆(H₂O)₂[Mo₈O₂₆] (1), Cu₅(pzta)₆(H₂O)₆[PW₁₂O₄₀]·(OH) (2), Cu₄(pzta)₂(bipy)(H₂O)₄(OH)₂[Mo₈O₂₆]·2H₂O (3) and [Cu₂(pzta)₂(bipy)₂(H₂O)₂][HPW₁₂O₄₀]·8H₂O (4) were obtained. The four compounds show distinct structure motifs from 3D self-penetrating framework to 1D poly-pendant chain, which illustrate that the POMs and the secondary spacers are key factors to tune the dimension of the POM-based inorganic-organic hybrids. Also, the luminescent and electrochemical properties for the title compounds are investigated.

Experimental Section

Materials and General Methods

All reagents were purchased commercially and were used without further purification. Elemental analyses (C, H and N) were performed on a Perkin-Elmer 2400 CHN Elemental Analyzer, and that of P, Cu, W and Mo were carried out with a Leaman inductively coupled plasma (ICP) spectrometer. The FT-IR spectra were recorded from KBr pellets in the range 4000–400 cm⁻¹ with a Nicolet AVATAR FT-IR360 spectrometer. A CHI660 electrochemical workstation was used for control of the

electrochemical measurements and data collection. A conventional three-electrode system was used, with a carbon paste electrode (CPE) as a working electrode, a commercial Ag/AgCl as reference electrode and a twisted platinum wire as counter electrode. The powder X-ray diffraction (PXRD) data were collected on a Rigaku RINT2000 diffractometer at room temperature. The photoluminescence analyses were carried out on an Edinburgh Fluorescence spectrometer at room temperature.

Synthesis of Cu₅(**pzta**)₆(**H**₂**O**)₂[**Mo**₈**O**₂₆] (1). A mixture of (NH₄)₆Mo₇O₂₄·4H₂O (0.37 g, 0.3mmol), CuCl₂·2H₂O (0.16 g, 0.9 mmol), pzta (0.12 g, 0.81 mmol) and water (15 mL) was stirred for 1h. The resulting solution was transferred to a Teflon lined autoclave and kept under autogenous pressure at 160 °C for 4 days. After slow cooling to room temperature, blue block crystals of **1** were filtered, washed with distilled water and dried at room temperature. Yield: 43 % (based on Mo). Anal. calcd. for C₃₀H₂₂N₃₆O₂₈Cu₅Mo₈: H, 0.92; C, 14.89; N, 20.84; Cu, 13.13; Mo, 31.72 %; Found: H, 0.97; C, 14.82; N, 20.89; Cu, 12.99; Mo, 31.81 %.

Cu₅(pzta)₆(H₂O)₆[PW₁₂O₄₀]·(OH) (2). The synthetic method was similar to that of compound 1, except that the (NH₄)₆Mo₇O₂₄·4H₂O was replaced by H₃PW₁₂O₄₀. Dark green block crystals of 2 were filtered, washed with water, and dried at room temperature. Yield: 49 % (based on W). Anal. calcd. for C₃₀H₃₁N₃₆O₄₇Cu₅PW₁₂: H, 0.74; C, 8.57; N, 12.00; P, 0.74; Cu, 7.56; W, 52.49 %; Found: H, 0.81; C, 8.62; N, 11.94; P, 0.79; Cu, 7.47; W, 52.41%.

Cu₄(pzta)₂(bipy)(OH)₂(H₂O)₄[Mo₈O₂₆]·2H₂O (3). Introducing 4, 4'-bipy (0.08 g, 0.42 mmol) into the reaction system of 1, blue block crystals of 3 were filtered,

washed with distilled water and dried at room temperature. Yield: 43 % (based on Mo). Anal. calcd. for $C_{20}H_{28}N_{14}O_{34}Cu_4Mo_8$: H, 1.39; C, 11.83; N, 9.66; Cu, 12.52; Mo, 37.80 %; Found: H, 1.34; C, 11.78; N, 9.72; Cu, 12.45; Mo, 37.89%.

[Cu₂(pzta)₂(bipy)₂(H₂O)₂][HPW₁₂O₄₀]·8H₂O (4). The synthetic method was similar to that of compound 3, except that the (NH₄)₆Mo₇O₂₄·4H₂O was replaced by H₃PW₁₂O₄₀. Dark green block crystals of 4 were filtered, washed with water, and dried at room temperature. Yield: 47% (based on W). Anal. Calcd. For C₃₀H₄₃ N₁₆O₅₀Cu₂ PW₁₂: H, 1.12; C, 9.50; N, 5.91; P, 0.82; Cu, 3.35; W, 58.20 %; Found: H, 1.06; C, 9.57; N, 5.85; P, 0.88; Cu, 3.28; W, 58.27%.

Table 1. Crystal Data and Structure Refinements for Compounds 1-4.

Compounds	1	2	3	4
Formula	$C_{30}H_{22}Cu_5Mo_8N_{36}O_{28}\\$	$C_{30}H_{31}Cu_5N_{36}O_{47}PW_{12} \\$	$C_{20}H_{28}Cu_{4}Mo_{8}N_{14}O_{34} \\$	$C_{30}H_{43}Cu_{2}N_{16}O_{50}PW_{12} \\$
Fw	2420.08	4221.61	2030.18	3791.79
T (K)	293(2)	293(2)	293(2)	293(2)
crystal system	Triclinic	Monoclinic	Triclinic	Triclinic
space group	P-1	C2/c	P-1	P-1
a (Å)	11.0152(5)	16.437(4)	10.7704(5)	12.191(5)
b (Å)	11.7744(5)	21.933(6)	11.2485(5)	13.180(5)
c (Å)	12.4173(6)	21.811(6)	12.3945(5)	13.506(5)
α (°)	70.921(1)	90	63.892(5)	92.714(5)
β(°)	86.690(1)	100.372(3)	66.121(4)	109.859(5)
γ(°)	89.694(1)	90	73.689(7)	110.756(5)
$V(\mathring{A}^3)$	1519.33(12)	7735.(4)	1223.26(9)	1873.6(1)
Z	1	4	1	1
D_c (g·cm ⁻³)	2.641	3.625	2.737	3.342
$\mu (\mathrm{mm}^{-1})$	3.414	19.246	3.788	19.015
Refl. Measured	10394	30966	9923	9411
Refl. Unique	5503	9676	6067	6592
$R_{ m int}$	0.0128	0.0873	0.0139	0.0302
F(000)	1155.0	7560.0	956.0	1675.0
R_1^a , wR_2^b	$R_1^{\ a} = 0.0198$	$R_1^{\ a} = 0.0857$	$R_1^{\ a} = 0.0268$	$R_1^{\ a} = 0.0715$
$[I > 2\sigma(I)]$	$wR_2^b = 0.0538$	$wR_2^b = 0.2419$	$wR_2^b = 0.0692$	$wR_2^b = 0.2044$
GOF on F^2	1.018	1.047	1.031	1.081

$${}^{a}R_{1} = \sum \|F_{o}\| - \|F_{c}\| / \sum \|F_{o}\|$$
. ${}^{b}wR_{2} = \{\sum [w(F_{o}^{2} - F_{c}^{2})^{2}] / \sum [w(F_{o}^{2})^{2}]\}^{1/2}$

X-ray Crystallography. Data collection for 1-4 were performed on a Bruker SMART Apex CCD diffractometer at 293(2) K. Absorption corrections were applied by using the multiscan program SADABS. 15 The structures were solved by direct methods, and non-hydrogen atoms were refined anisotropically by least-squares on F² using the SHELXTL program. 16 The hydrogen atoms of organic ligands were generated geometrically for 1-4, while the hydrogen atoms of water molecules can not be found from the residual peaks and were directly included in the final molecular formula. The centre oxygen atoms in PO₄ group of Keggin clusters are disordered by symmetry in compounds 2 and 4, which is usual for Keggin structures, and the occupied factors of these disordered centre oxygen atoms (O11, O12, O13 and O14 atoms for 2, O12, O24, O25 and O26 atoms for 4 atoms) are 0.5. A summary of the crystal data, data collection, and refinement parameters for 1-4 are listed in Table 1. Crystallographic data for the structures reported in this paper have been deposited in the Cambridge Crystallographic Data Center with CCDC Number: 948523 for 1, 948524 for **2**, 948525 for **3** and 948522 for **4**.

Results and Discussion

All the $[Mo_8O_{26}]^{4-}$ clusters in **1** and **3** are a typical β -octamolybdate, which exhibits the most compact structure of eight edge-sharing $[MoO_6]$ octahedra with two $[Mo_4O_{13}]$ subunits stacking together.¹⁷ All the $[PW_{12}O_{40}]^{3-}$ polyanions in **2** and **4** exhibit a classical α -Keggin configuration: the central atoms P are disordered surrounded by a

cube of eight oxygen atoms with each oxygen site half occupied; the bond lengths and bond angles both are in the normal ranges.¹⁸ All tungsten and molybdenum atoms are in +VI oxidation states, and copper atoms are in +II oxidation states in compounds **1–4**, which was confirmed by charge neutrality, coordination environments and valence sum calculations.¹⁹

Structure Description of Compound 1

Single-crystal X-ray diffraction analysis reveals that the structure of **1** is a 3D inorganic-organic hybrid constructed by 2D Cu-pzta layers and $[\beta-(Mo_8O_{26})Cu(pzta)_2]_n$ chain. The asymmetric unit of **1** consists of one $\beta-[Mo_8O_{26}]^4$ anion (abbreviated as $\beta-Mo_8$), five cooper ions, six pzta ligands and two H₂O molecules (Fig. 1).

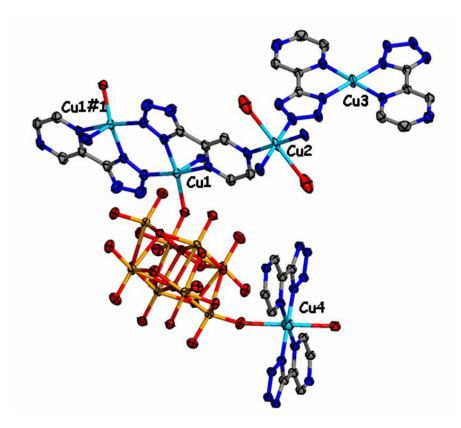


Fig. 1 An **OPTEP** drawing of the basic crystallographic unit in **1** at the 50% probability and showing the coordination environments around the Cu atoms. (All the hydrogen atoms are omitted for clarity). (Symmetry code: #1, 2-x, 1-y,-z.)

There are four crystallographically independent Cu ions with three kinds of coordination modes (Figure 1). Cu1 is five-coordination in rectangular pyramidal coordination geometry ($\tau = 0.237$)²⁰ achieved by one oxygen atom from the β -Mo₈ anion and four nitrogen atoms from three pzta ligands. Both Cu2 and Cu4 are

six-coordination in distorted octahedral geometries, but their coordination environments are entirely different. The Cu2 is coordinated by two oxygen atoms from two water molecules and four nitrogen atoms from two pzta ligands. The Cu4 is coordinated by two oxygen atoms from two β -Mo₈ anions and four nitrogen atoms from two pzta ligands. Cu3 is four-coordination in square-planar geometry achieved by four nitrogen atoms from two pzta ligands. The bond lengths and angles around the Cu ions are in the ranges of 1.943(3)-2.196(3) Å (Cu-N), 2.014(2)-2.373(2) Å (Cu-O), $80.62(11)-180.00(1)^{\circ}$ (N-Cu-N) and $80.14(9)-99.86(9)^{\circ}$ (N-Cu-O). The coordination fashion of the six pzta ligands can be divided into two kinds: $\mu_{1,2,3}$ and $\mu_{1,2,4}$ (Scheme 1). All of these bond lengths and bond angles are within the normal ranges observed in other Cu(II)-containing complexes.²¹ As a result, two kinds of complexes are formed: (i) two pzta ligands chelate two Cu1 centers leading to Cu₂(pzta)₂ subunit (subunit-A); (ii) two pzta ligands chelate one Cu₃ or Cu₄ center forming Cu(pzta)₂ subunit (subunit-B or subunit-C) (Fig. S1). The neighboring subunit-A is connected by Cu2 (Cu2-N1 bonds) to form an infinite coordination polymer chain (Fig. S2a). Furthermore, these adjacent chains are linked together by subunit-B to generate a 2D Cu-pzta layer, in which rectangular windows are formed with effective size of $16.17 \times 11.77 \text{ Å}^2$ (Fig. S2b). The β -Mo₈ anions and subunit-C are linked alternately by Cu4–O7 bonds forming an [β-(Mo₈O₂₆)Cu(pzta)₂]_n organic-inorganic hybrid chain (Fig. S3). Finally, the chains are inserted into the rectangular windows of 2D Cu-pzta layers. Consequently, the chains and the 2D layers are incorporated via Cu1-O13 bonds to give birth to a complicated 3D

structure (Fig. 2).

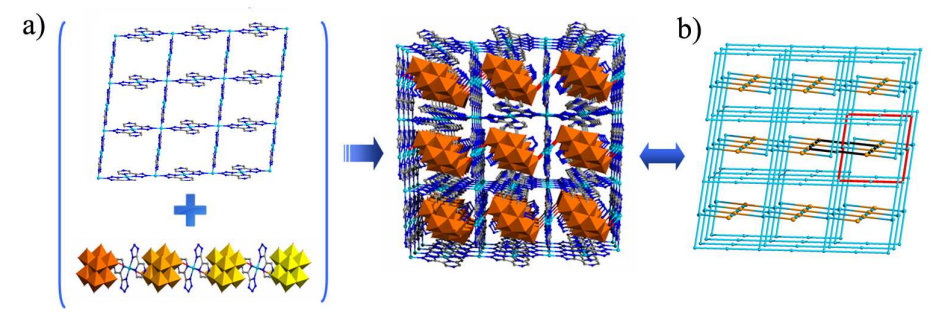


Fig. 2 Illustration of the unique 3D self-penetrating (3, 4, 4)-connected net of 1.

From the topological view, if each subunit B/C is considered as a 2-connected nodes, the Cu1 cation act as a 3-connected node, Cu2 cation and the β -Mo₈ anions act as 4-connected nodes, the structure of **1** is a novel self-penetrating (3, 4, 4)-connected framework with $(10^2 \cdot 12^1)$ $(9^3 \cdot 10^2 \cdot 14^1)$ $(9^2 \cdot 10^2 \cdot 11^1 \cdot 14^1)_2$ topology (Fig. 2, Fig. S4). In fact, a few self-penetrating nets have been observed in hybrids,²² and the self-penetrating POMs-based hybrids are even rarer.^{17a, 23} To the best of our knowledge, this framework represents the first 3D self-penetrating structure assembly from pzta ligands.

Structure Description of Compound 2 Crystal structure analysis reveals that the structure of **2** is a POM-templated 2D inorganic-organic hybrid, which is formed by a 2D copper-pzta framework with square windows incorporated $[PW_{12}O_{40}]^{3-}$ (PW_{12}) templates. The asymmetric unit of **2** consists of one PW_{12} polyoxoanion, five copper ions, six pzta ligands, six coordinated water molecules and one hydroxyl (Fig. 4).

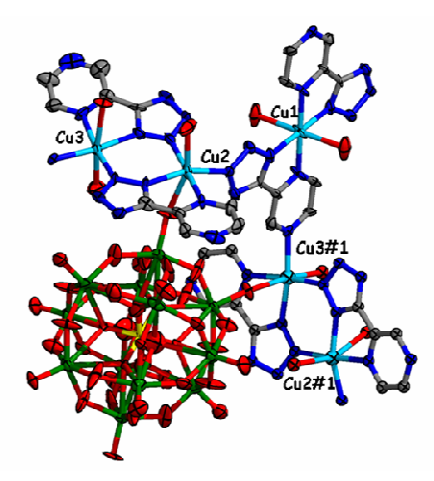


Fig. 3 An **OPTEP** drawing of the basic crystallographic unit in **2** at the 50% probability and showing the coordination environments around the Cu atoms. (All the hydrogen atoms are omitted for clarity). (Symmetry code: #1, x, 1-y,-0.5+z.)

There are three crystallographically independent Cu ions with six-coordination modes in distorted octahedral geometries (Fig. 3). But their coordination environments are entirely different. Cu1 is coordinated by two oxygen atoms from two water molecules, four nitrogen atoms from two pzta ligands. Cu2 and Cu3 are coordinated by two oxygen atoms from a water molecule and a PW₁₂ polyoxoanion and four nitrogen atoms from three pzta ligands. The bond lengths and angles around the Cu ions are in the ranges of 1.951(18)–2.077(19) Å (Cu–N), 2.33(2)–2.38(2) Å (Cu–O), 79.9 (8)–180.0(7)° (N–Cu–N) and 85.3(7)–108.2(9)° (N–Cu–O). All of these bond lengths are within the normal ranges observed in other Cu(II)-containing complexes.²¹ Two kinds of pzta ligands exist in the $\mu_{1,2,3}$ and $\mu_{1,2,4,6}$ coordination modes in the structure (Scheme 1). As a result, two kinds of TMCs are formed (Fig. 4a): (i) two pzta ligands chelate one Cu1 center forming Cu(pytz)₂ subunit (subunit-A); (ii) two pzta ligands chelate Cu2 and Cu3 centers while Cu2 and Cu3 centers link nitrogen atom in the pyridine ring of the other ligand leading to Cu₂(pzta)₂ subunit (subunit-B). Subunit-A

and subunit-B are linked alternately by Cu2–N2 and Cu3–N7 bonds to form a 2D layer showing a square window with effective size of 15.47×15.47 Å² (Fig. 4b). Interestingly, the PW₁₂ polyanions acting as templates are encapsulated into the square windows and connect the copper-pzta framework *via* sharing the oxygen atoms (Fig. 4c). From the topological view, if each the Cu2/Cu3 cation is considered as 3-connected nodes, subunits A and PW₁₂ polyoxoanions act as a 4-connected nodes, the structure of **2** is a novel (3, 3, 4, 4)-connected 2D framework with $(4^1 \cdot 6^2)_2$ $(4^2 \cdot 6^2 \cdot 8^2)_2$ topology (Fig. 4d).

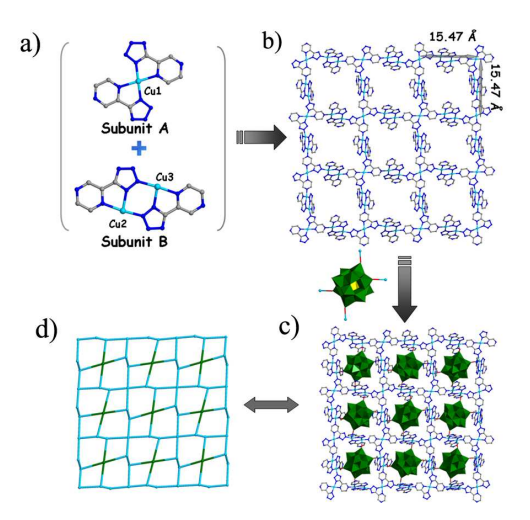


Fig. 4 Ball/stick representation of subunit A, subunit B, 2D layer formed by subunit A and B, and the topology of 2D layer in **2**.

Structure Description of Compound 3 Single-crystal X-ray diffraction analysis reveals that **3** shows a 2D layer structure, which is constructed by β -Mo₈ anions and 1D chain formed by tetranuclear copper units and bipy molecule.

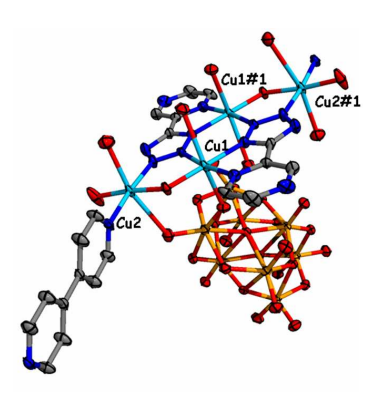


Fig. 5 An **OPTEP** drawing of the basic crystallographic unit in **3** at the 50% probability and showing the coordination environments around the Cu atoms. (All the hydrogen atoms are omitted for clarity). (Symmetry codes: #1, 1-x, 1-y, -z.)

As shown in Fig. 5, there are two crystallographically independent Cu ions with six-coordination modes in 3. But their coordination environments are entirely different. Cu1 is coordinated by three oxygen atoms from one hydroxyl group and two the β -Mo₈ anions, three nitrogen atoms from two pzta ligands. Cu2 is coordinated by four oxygen atoms from two coordinated water molecules, one hydroxyl group and one β -Mo₈ anion, two nitrogen atoms from one pzta ligand and one bipy ligand. The bond lengths and angles around the Cu ions are in the ranges of 1.965(6)-2.061(6) Å 1.873(5)-2.392(5) Å (Cu-O), 79.8(2)-172.9(2)° (N-Cu-N)83.6(2)-99.1(2)° (N-Cu-O). Due to the introducing of bipy molecule into the reaction system, there exists competitive reaction between the bipy and pzta molecules. The pzta ligands exist only one $\mu_{1,2,3}$ coordination modes in the structure (Scheme 1). The two kinds of Cu ions are linked together via pzta forming a tetranuclear copper unit (Fig. 6a). And these tetranuclear copper units are connected by bipy molecules to form a chain (Fig. 6b). Further, these adjacent chains are fused together by six connected β-Mo₈ anions to achieve a layer with 18.51×12.87 Å² voids

(Fig. 6c). As is known, large structural voids are often occupied by solvent molecules or guest molecules to achieve the structural stabilization. Otherwise, the interpenetration phenomena may occur, that is, the voids associated with one framework are occupied by one or more independent frameworks to fill the spaces. Interestingly, in the structure of compound 3, these layers are occupied by the protrudent pzta ligands from the adjacent layers to forming a 2D + 2D \rightarrow 3D interdigitated architecture (Fig. 7, Fig. S5). Complementary intermolecular hydrogen bondings existing between the two adjacent layers stabilize this structure (typical hydrogen bondings: O2-C7 = 3.09 Å, O3-C4 = 3.25 Å, O9-C7 = 3.17 Å, O10-C10= 3.12 Å and O13-C5 = 3.23 Å). To the best of our knowledge, only two POM-based interdigitatied compounds have been reported up to now.²⁴ And the two interdigitatied compounds are respectively constructed from the vanadate and Keggin clusters. Therefore, compound 3 represents the first exceptional case assembled from octamolybdate clusters and tetranuclear copper units. From the topological view, if each the Cu2 cation, Cu1 cation and β -Mo₈ anion is considered as 3-connected nodes, 4-connected nodes and 6-connected nodes, respectively, the structure of 3 is a (3, 4, 6)-connected 2D framework with $(3^1 \cdot 8^2) (3^3 \cdot 4^2 \cdot 6^1) (3^4 \cdot 4^2 \cdot 8^2 \cdot 9^4 \cdot 10^3)$ topology (Fig. 6d).

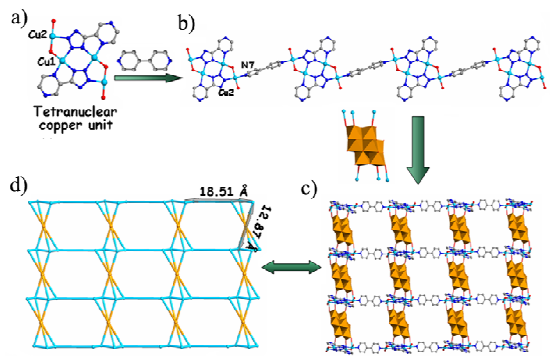


Fig. 6 View of (a) tetranuclear copper unit, (b) chain formed by tetranuclear copper unit and bipy molecular, (c) 2D MOFs formed by β-Mo₈ anions and (d) the topology of 2D layers.

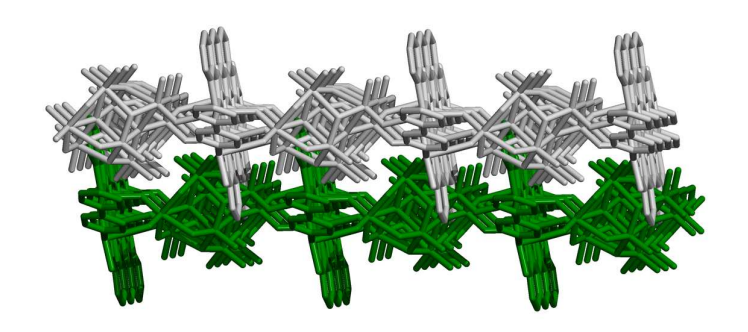


Fig. 7 View of the $2D + 2D \rightarrow 3D$ interdigitated architecture in 3.

Structure Description of Compound 4 Single-crystal X-ray diffraction analysis reveals that **4** is constructed by PW_{12} Keggin clusters and $[Cu(pzta(bipy)(H_2O)]_2$ dinuclear copper complexes (Fig. 8). For the charge balance, a proton is added to the PW_{12} clusters, as also observed in $[Ag_2(3atrz)_2]_2[(HPMo^{VI}_{10}Mo^{V}_2O_{40})]^{.25}$

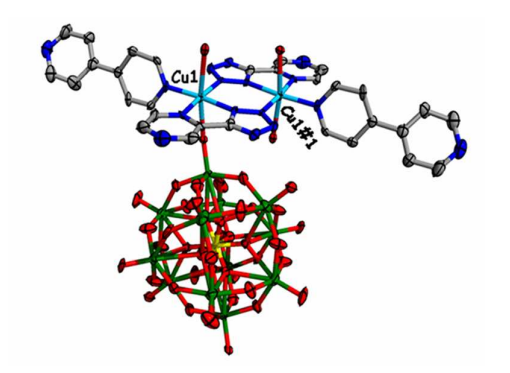


Fig. 8 An **OPTEP** drawing of **4** at the 50% probability level showing the coordination environments around the Cu atoms. (All the hydrogen atoms are omitted for clarity). (Symmetry codes: #1, 1-x, -y, -z.)

There are one crystallographically unique Cu center and it shows a six-coordination distorted octahedral geometry achieved by three N atoms from two pzta ligands, two O atoms from one PW₁₂ cluster and one water molecule. The bond lengths and angles around the Cu ions are in the ranges of 1.974(17)–2.065(19) Å (Cu–N), 2.364(16) Å (Cu–O), 80.4(7)–173.3(7)° (N–Cu–N) and 87.0(6)–95.2(7) (N–Cu–O). By these coordination mode, the two adjacent symmetrical Cu ions are linked together *via* pzta

and bipy ligands forming a [Cu(pzta(bipy)(H₂O)]₂ dinuclear copper complexes. In addition, each of the PW₁₂ cluster acts as a didentate inorganic ligand coordinating with two copper centers from the two dinuclear copper complexes. Thus, these complexes are further connected by PW₁₂ clusters to form a 1D poly-pendant chain via Cu1–O8 (2.364 Å) bonds (Fig. S6), in which the mono-coordinated bipy molecules as pendant ligands are appended to the two sides of the chain. Further, these adjacent chains are fused together forming a porous 2D layer via π – π interactions between the two neighboring mono-coordinated bipy pendants (Fig. 9).

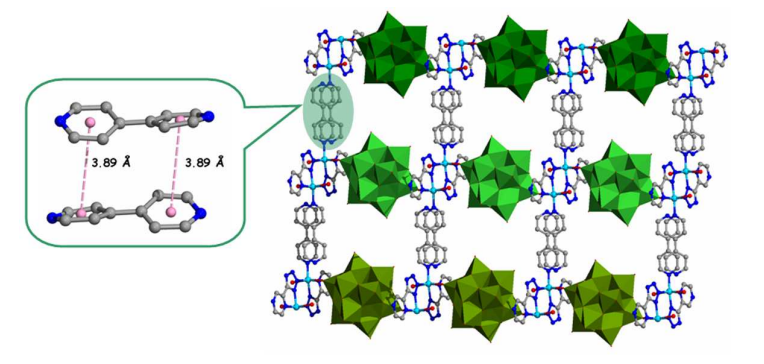


Fig. 9 Combined polyhedral/ball/stick representation of the 2D layer via π - π interactions.

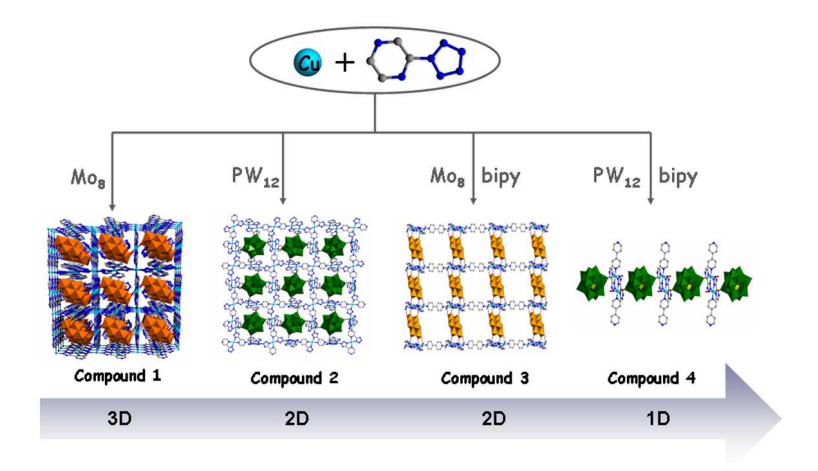
Influence of the different POM clusters and secondary spacer on structure of POM-based inorganic-organic hybrids.

The secondary spacer is known to be an important factor in the modification of the structure of inorganic-organic hybrids. However, such an effect is seldom considered in the assembly of POM-based inorganic-organic hybrids, due to the difficulty to control the self-assembly processes. In this work, through changing the POM clusters and/or introducing secondary spacers, we have achieved the alternation of dimensionality to observe the effect of POM clusters and secondary spacers on the POM-based inorganic-organic hybrids assembly (Scheme 2). First of all, we study the

influence of the polyanions on the structures of compounds. As compounds 1 and 2 were synthesized under the identical reaction conditions, except for alternation of the polyoxoanions (β -Mo₈ for 1 and PW₁₂ for 2), we deduce that the influence of the polyoxoanions on the final structures of 1 and 2 may arise from the differences in their volumes. Compound 1 is constructed by 2D Cu-pzta layers with rectangular (16.17)11.77 $Å^2$) and infinite inorganic-organic windows $[\beta-(Mo_8O_{26})Cu(pzta)_2]_n$. The $[\beta-(Mo_8O_{26})Cu(pzta)_2]_n$ chains containing smaller dimensions of the β -Mo₈ clusters (ca. 10.18 × 6.27 Å) are aslant inserted into the rectangular windows of 2D Cu-pzta layers and are further incorporated to form a self-penetrating 3D framework. However, compound 2 is a POM-templated 2D layer structure, which constructed by 2D Cu-pzta layer with square window (15.47×15.47 $Å^2$) and the spherical diameter of the PW₁₂ template (ca. 10.45 Å).

To investigate influence of the secondary spacer on structures of the POM-based inorganic-organic hybrids structure, the linear rigid bipy molecule is introduced into the reaction system of 1 and 2, respectively, and 3 and 4 were obtained. As a result, the dimensionality frameworks of compounds 3 and 4 are lower than that of the 1 and 2 respectively. Namely, the structure of 3 shows a 2D layer that consists of the adjacent metal-organic chains fused together by six connected β -Mo₈ anions, and 4 exhibits a 1D poly-pendant chain constructed by dinuclear copper complexes and PW₁₂ clusters (Scheme 2). The possible reasons for such phenomenon are as following: Firstly, all of the compounds possess the dinuclear or polynuclear copper complexes with multiple

coordination sites showing radiation coordination modes are in favor of forming high-dimensional framework. However, in 3 and 4, the bipy molecules with big steric hindrance as secondary spacers are introduced into the reaction systems and connected with the copper atoms of the dinuclear or polynuclear complexes, to some extent, reducing the radiation coordination modes of dinuclear or polynuclear complexes. Additionally, compared with the pzta possessing six potential N-coordination sites (Scheme 1), the 4,4'-bipy molecule that only contains two terminal pyridyl groups in the opposite positions, which is also a negative factor to form complicated structures.



Scheme 2. Summary of the influences of the different POM clusters and secondary spacer on the structures of **1-4**.

Analyses of IR spectra and PXRD

As shown in Fig. S7, the IR spectra exhibit the characteristic peaks at 945, 891, 797 and 677 cm⁻¹ in **1**; 941, 889, 786 and 681 cm⁻¹ in **3**, which are attributed to v(Mo=Ot) and $v_{as}(\text{Mo-Oc-Mo})$, respectively. Comparing the IR spectra of **1** and **3** with that of β -Mo₈ anions, ²⁶ it can be observed that the shape of peaks in the range 600-1000 cm⁻¹ is nearly identical to that of β -Mo₈ anions except slight shifts of some peaks due to the

effect of coordination. The IR spectra exhibit the characteristic peaks at 1051, 945, 881 and 790 cm⁻¹ in **2**; 1053, 946, 883 and 789 cm⁻¹ in **4**, which are attributed to v(P-O), v(W=Ot), $v_{as}(W-Ob-W)$ and $v_{as}(W-Oc-W)$, respectively. Compared to the typical α -Keggin-type heteropolyanion PW_{12} , ²⁷ these results indicate that the polyoxoanions in **2** and **4** are distorted due to the interaction between heteropolyanion PW_{12} and copper-organonitrogen coordination polymer. Additionally, the bands in the region of 1601 to 1127 cm⁻¹ could be ascribed to the character peaks of pzta ligands in **1** and **3** as well as pzta and/or 4, 4'-bipy ligands in **2** and **4**. The peak at 3451, 3435, 3432 and 3442 can be assigned to the vibrations of water molecules in **1–4**, respectively.

As shown in Fig. S8, the X-ray powder diffraction patterns measured for the as-synthesized samples of **1–4** are all in good agreement with the PXRD patterns simulated from the respective single-crystal X-ray data, proving the purity of the bulk phases.

Photoluminescent properties

Luminescent compounds are of great current interest for various potential applications.²⁸ Therefore the photoluminescence properties of **1–4** are investigated in the solid state at room temperature (see Fig. 10). It is clear that there is one similar emission peaks at ca. 468 nm ($\lambda_{ex} = 368$ nm) for **1**, 474 nm ($\lambda_{ex} = 373$ nm) for **2**, 436 nm ($\lambda_{ex} = 349$ nm) for **3** and 431 nm ($\lambda_{ex} = 343$ nm) for **4**, respectively. In order to understand the nature of the luminescence, the emission spectra of free pzta and bipy ligands were also investigated under identical experimental conditions. The free bipy

exhibits no photoluminescence which is consist with the previous report, ²⁹ whereas the free pzta shows intense emission peaks at ca. 454 nm upon excitation at 359 nm (Fig. S9). Obviously, the emission of 1–4 is similar with free pzta ligand. Compared to the free pzta ligand, the emission spectra of 1 and 2 are red-shifted, while that of 3 and 4 are blue-shifted. Therefore, the origin of the emission of 1–4 can be tentatively attributable to ligand (pzta)-to-metal (Cu^{II}) charge transfer (LMCT). ³⁰ The red-shift of 1 and 2 compared to the free pzta ligands may be due to the coordination of pzta ligands with Cu^{II} ions. The blue-shift of 3 and 4 compared to the free pzta ligand may be due to the introducing secondary spacer bipy molecule into pzta ligands and Cu ions system. ³¹ Since 1–4 are insoluble in common polar and nopolar solvents, they may be good candidates for potential solid-state luminescent materials.

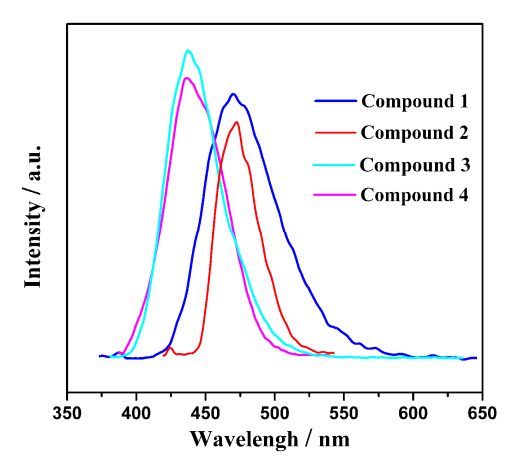


Fig. 10 The emission spectra of compounds 1-4.

Cyclic Valtammetry (CV)

Title complexes are insoluble in water and common organic solvents. Thus, the bulk-modified carbon paste electrode (CPE) becomes the optimal choice to study the electrochemical properties, which is inexpensive, easy to prepare and handle.

The electrochemical behaviors of the 1- and 2-CPEs are respectively similar to the 3- and 4-CPEs, and thus the 1- and 2-CPEs have been taken as examples to study their electrochemical properties. The electrochemical behaviors were studied in 1M H₂SO₄ solution at the scan rate of 50 mV·s⁻¹. For 1-CPE, as shown in Fig. S10 (left), it can be seen that there is one pairs of quasi-reversible redox peaks (II-II') appeared in the potential range +0.2 to -0.4 V, and the mean peak potentials $E_{1/2} = (E_{pa} + E_{pc})/2$ is -0.015 V, which can be ascribed to redox processes of Mo^{VI}/Mo^{V.32} For **2-**CPE, as shown in Fig. S10 (right), in the potential range +0.2 to -0.6 V, it can be seen that there are three pairs of reversible redox peaks with the mean peak potentials $E_{1/2}\!\!=\!\!(E_{pa}\!\!+E_{pc})\!/2$ are -0.098 (II-II'), -0.237 (III-III') and -0.573V (IV-IV'), which can be ascribed to redox processes of WVI/WV.33 In addition, there exist one pair of quasi-reversible anodic peaks (I-I') with the mean peak potentials +0.49 V for 1-CPE and +0.42V for 2-CPE, which are attributed to the redox processes of the Cu^{II} centers.³⁴ The different redox peaks of Cu-centers for the both CPEs may be abscribed to the subtle structural differences of compounds 1 and 2, which is consist with the previous work.^{24b, 35}

The electrocatalytic properties of **1-** and **2-**CPE have also been investigated. The results show that the **2-**CPE has no obvious electrocatalytic activities for hydrogen peroxide (H₂O₂) and ascorbic acid (AA) (Fig. S11), however, **1-**CPE possesses bifunctional electrocatalytic activities towards not only reduction of normal inorganic molecules H₂O₂ ascribed to Mo-centers, but also oxidation of biologic molecules AA ascribed to Cu-centers, which are seldom reported in the literature.^{35a, 36} As shown in

Fig. 11a, with addition of H_2O_2 , the reduction peak currents for II increase gradually while the corresponding oxidation peak currents decrease. While, with addition of AA, the anodic peak current of Cu(II) wave substantially increases, suggesting that 1 can electrically catalyze the oxidation of AA. The nearly equal current steps for each addition of H_2O_2 and AA demonstrate stable and efficient electrocatalytic activity of 1-CPE (see the insert figures of fig. 11 a and b).

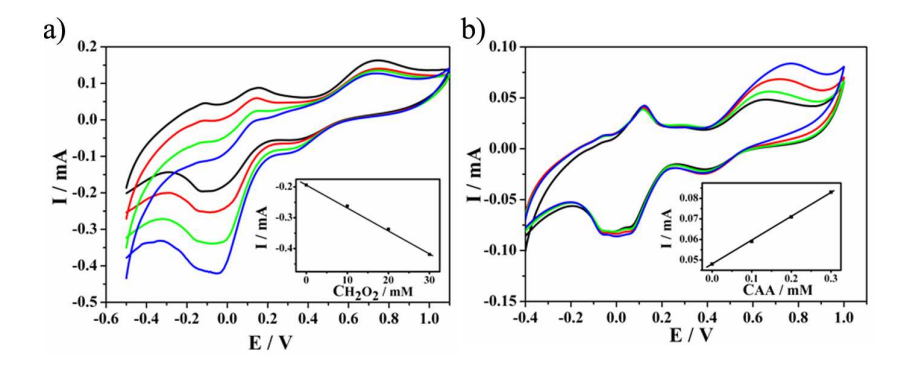


Fig. 11 (a) Reduction of H₂O₂ and (b) oxidation of AA for **1**-CPE, in 1M H₂SO₄ solution (scan rate: 0.50 mV·s⁻¹). The concentrations (from inner to outer) are 0.0, 10, 20, 30 mM for H₂O₂ and 0.0, 0.1, 0.2, 0.3 mM for AA. The inset shows a linear dependence of the cathodic catalytic current of wave II with H₂O₂ concentration and wave I with AA concentration, respectively.

Conclusions

In summary, four POM-based inorganic-organic hybrids compounds showing novel structure motifs from 3D self-penetrating framework to 1D poly-pendant chain have been synthesized under hydrothermal conditions. The isolation of **1-4** not only provides intriguing examples of POM-based inorganic-organic hybrids, but also shows that both POMs and the secondary spacers are key factors to tune the dimension of the inorganic-organic hybrids. The work represents one of the rare reports on that the secondary spacer is introduced into the frameworks of POM-based

inorganic-organic hybrids in order to modulate the structures of inorganic-organic hybrids. To some extent, our attempts will deepen systematic understanding the influences of POM clusters and secondary spacers on the assembly processes in hydrothermal conditions.

Acknowledgments

This work was financially supported by the NSF of China (No.21371041 and 21101045), the NSF of Heilongjiang Province (No.B201103), the Foundation of Education Committee of Heilongjiang (No.12521072), the Science and Technology Innovation Foundation of Harbin (No.2013RFQXJ144), the Excellent Academic Leader Program of HUST, and The SF for the Young Innovative Talents of HUST (No.201307) for the financial support.

References

(1) (a) H. K. Chae, D. Y. Siberio-Pérez, J. Kim, Y. Go, M. Eddaoudi, A. J. Matzger, M. O'Keeffe and O. M. Yaghi, *Nature*, 2004, 427, 523; (b) M. Eddaoudi, D. B. Moler, H. L. Li, B. L. Chen, T. M. Reineke, M. O'Keeffe and O. M. Yaghi, *Acc. Chem. Res.*, 2001, 34, 319; (c) S. R. Battan and K. S. Murray, *Coord. Chem. Rev.* 2003, 246, 103; (d) A. R. Millward and O. M. Yaghi, *J. Am. Chem. Soc.*, 2005, 127, 17998; (e) M. Kondo, T. Yoshitomi, K. Seki, H. Matsuzaka and S. Kitagawa, *Angew. Chem., Int. Ed.*, 1997, 36, 1725; (f) N. L. Rosi, J. Eckert, M. Eddaoudi, D. T. Vodak, J. Kim, M. O 'Keeffe and O. M. Yaghi, *Science*, 2003, 300, 1127; (g) T.

- K. Holman, Angew. Chem., Int. Ed.. 2011, 50, 1228.
- (2) (a) O. M. Yaghi, M. O 'Keeffe, N. W. Ockwig, H. K. Chae, M. Eddaoudi and J. Kim, Nature, 2003, 423, 705; (b) J. L. C. Rowsell, E. C. Spencer, J. Eckert, J. A. K. Howard, O. M. Yaghi and Science, 2005, 309, 1350; (c) C. G. Bezzu, M. Helliwell, J. E. Warren, D. R. Allan and N. B. McKeown, Science, 2010, 327, 1627; (d) L. Carlucci, G. Ciani and D. M. Proserpio, Coord. Chem. Rev., 2003, 246, 247; (e) Q. Li, C. H. Sue, S. Basu, A. K. Shveyd, W. Zhang, G. Barin, L. Fang, A. A. Sarjeant, J. F. Stoddart and O. M. Yaghi, Angew. Chem., Int. Ed., 2010, 49, 6751; (f) W. H. Fang, L. Cheng, L. Huang and G. Y. Yang, Inorg. Chem., 2013, 52, 6.
- (3) (a) P. J. Hagrman, D. Hagrman and J. Zubieta, *Angew. Chem., Int. Ed.*, 1999, 38, 2638; (b) A. Müller, M. T. Pope, F. Peters and D. Gatteschi, *Chem. Rev.*, 1998, 98, 239; (c) B. K. Won, T. Voitl and G. J. RodriguezRivera, J. A. Dumesic, Science, 2004, 305, 1280; (d) B. Z. Lin and S. X. Liu, *Chem. Commun.*, 2002, 2126; (e) T. McGlone, J. Thiel, C. Streb, D. L. Long and L. Cronin, *Chem. Commun.*, 2012, 48, 359; (f) S. Uchida, R. Eguchi and N. Mizuno, *Angew. Chem., Int. Ed.*, 2010, 49, 9930; (g) X. K. Fang, P. Kögerler, L. Isaacs, S. Uchida and N. Mizuno, *J. Am. Chem. Soc.*, 2009, 131, 432; (h) A. Dolbecq, E. Dumas, C. R. Mayer and P. Mialane, *Chem. Rev.*, 2010, 110, 6009; (i) D. Y. Du, L. K. Yan, Z. M. Su, S. L. Li, Y. Q. Lan and E. B. Wang, *Coord. Chem. Rev.*, 2013, 257, 702; (j) J. Song, Z. Luo, D. K. Britt, H. Furukawa, O. M. Yaghi, K. I Hardcastle and C. L. Hill, *J. Am. Chem. Soc.*, 2011, 133, 16839; (k) Q. X. Han, C. He, M. Zhao, B. Qi, J. Y. Niu

- and C. Y. Duan, J. Am. Chem. Soc., 2013, 135,10186.
- (4) (a) A. Müller, P. Kögerler and C. Kuhlmann, Chem. Commun., 1999, 13 47; (b) A. Müller, C. Beugholt, M. Koop, S. K. Das, M. Schmidtmann and H. Z. Bögge, Anorg. Allg. Chem., 1999, 625, 1960; (c) G. J. T. Cooper and L. Cronin, J. Am. Chem. Soc., 2009, 131, 8368; (d) S. T. Zheng, J. Zhang and G. Y. Yang, Angew. Chem., Int. Ed., 2008, 47, 1; (e) H. Y. An, E. B. Wang, D. R. Xiao, Y. G. Li, Z. M. Su and L. Xu, Angew. Chem., Int. Ed., 2006, 45, 904; (f) P. Kögerler and L. Cronin, Angew. Chem., Int. Ed., 2005, 44, 844; (g) A. Müller and C. Serain, Acc. Chem. Res., 2000, 33, 2; (h) T. McGlone, C. Streb, M. Busquets-Fite, J. Yan, D. Gabb, D. L. Long and L. Cronin, Cryst. Growth Des., 2011, 11, 2471; (i) C. Streb, R. Tsunashima, D. A. MacLaren, T. McGlone, T. Akutagawa, T. Nakamura, A. Scandurra, B. Pignataro, N. Gadegaard and L. Cronin, Angew. Chem., Int. Ed., 2009, 48, 6490; (j) E. F. Wilson, H. Abbas, B. J. Duncombe, C. Streb, D. L. Long and L. Cronin, J. Am. Chem. Soc., 2008, 130, 13876.
- (5) (a) A. Müller, E. Beckmann, H. Bögge, M. Schmidtmann and A. Dress, *Angew. Chem., Int. Ed.*, 2002, 41, 1162; (b) N. Mizuno, K. Yamaguchi and K. Kamata, *Coord. Chem. Rev.*, 2005, 249, 1944; (c) M. Wei, C. He, M. Hua, C. Y. Duan, S. Li and Q. J. Meng, *J. Am. Chem. Soc.*, 2006, 128, 13318; (d) Y. Q. Lan, S. L. Li, Z. M. Su, K. Z. Shao, J. F. Ma, X. L. Wang and E. B. Wang, *Chem. Commun.*, 2008, 58; (e) Y. M. Xie, Q. S. Zhang, Z. G. Zhao, X. Y. Wu, S. C. Chen and C. Z. Lu, *Inorg. Chem.* 2008, 47, 8086; (f) S. T. Zheng and G. Y. Yang, *Chem. Soc. Rev.*, 2012, 41, 7623.

- (6) For some examples on POM-based hybrids aspects, see (a) C. P. Pradeep, D. L. Long and L. Cronin, *Dalton Trans.*, 2010, 39, 9443; (b) P. P. Zhang, J. Peng, H. J. Pang, J. Q. Sha, M. Zhu, D. D. Wang, M. G. Liu and Z. M. Su, *Cryst. Growth Des.*, 2011, 11, 2736; (c) F. J. Ma, S. X. Liu, C. Y. Sun, D. D. Liang, G. J. Ren, F. Wei, Y. G. Chen and Z. M. Su, *J. Am. Chem. Soc.*, 2011, 133, 4178; (d) X. L. Wang, H. L. Hu, A. X. Tian, H. Y. Lin and J. Li, *Inorg. Chem.*, 2010, 49, 10299; (e) X. J. Kong, Y. P. Ren, P. Q. Zheng, Y. X. Long, L. S. Long, R. B. Huang and L. S. Zheng, *Inorg. Chem.*, 2006, 45, 10702; (f) G. F. Hou, L. H. Bi, B. Li and L. X. Wu, *Inorg. Chem.*, 2010, 49, 6474; (g) D. B. Dang, Y. Bai, C. He, J. Wang, C. Y. Duan and J. Y. Niu, *Inorg. Chem.*, 2010, 49, 1280; (h) Z. M. Zhang, Y. G. Li, Y. H. Wang, Y. F. Qi and E. B. Wang, *Inorg. Chem.*, 2010, 49, 11644; (i) J. W. Zhao, J. Zhang, S. T. Zheng and G. Y. Yang, *Chem. Commun.*, 2008, 570.
- (7) (a) E. Burkholder, V. Golub, C. J. O'Connorr and J. Zubieta, *Inorg. Chem.*, 2004, 43, 7014; (b) Z. Y. Shi, J. Peng, C. J. Gómez-García, S. Benmansour and X. J. Gu, *J. Solid State Chem.*, 2006, 179, 253; (c) Y. Q. Lan, S. L. Li, K. Z. Shao, X. L. Wang and Z. M. Su, *Dalton Trans.*, 2008, 3824.
- (8) (a) T. M. Anderson, W. A. Neiwert, K. I. Hardcastle and C. L. Hill, *Inorg. Chem.*, 2004, 43, 7353; (b) C. Zhang, R. C. Howell, K. B. Scotland, F. G. Perez, L. Todaro and L. C. Francesconi, *Inorg. Chem.*, 2004, 43, 7691.
- (9) (a) A. X. Tian, J. Ying, J. Peng, J. Q. Sha, Z. G. Han, J. F. Ma, Z. M. Su, N. H. Hu and H. Q. Jia, *Inorg. Chem.*, 2008, 47, 3274; (b) A. X. Tian, J. Ying, J. Peng, J. Q. Sha, H. J. Pang, P. P. Zhang, Y. Chen, M. Zhu and Z. M. Su, *Cryst. Growth Des.*,

2008, **8**, 3717.

- (10) (a) Y. T. Wang, M. L. Tong, H. Fan, H. Z. Wang and X. M. Chen, *Dalton Trans.*,
 2005, 424. (b) R. Mondal, M. K. Bhunia and K. Dhara, *CrystEngComm.*, 2008,
 10, 1167; (c) C. Y. Niu, B. L. Wu, X. F. Zheng, H. Y. Zhang, H. W. Hou, Y. Y.
 Niu and Z. J. Li, *Cryst. Growth Des.*, 2008, 8, 1566.
- (11) (a) E. Fournier, F. Lebrun, M. Drouin, A. Decken and P. D. Harvey, *Inorg. Chem.*, 2004, 43, 3127; (b) E. Q. Gao, S. Q. Bai, Z. M. Wang and C. H. Yan, Dalton Trans., 2003, 1759.
- (12) (a) J. Tao, X. M. Zhang, M. L. Tong and X. M. Chen, J. Chem. Soc., Dalton Trans., 2001, 770. (b) C. Z. Lu, C. D. Wu, H. H. Zhuang and J. S. Huang, Chem. Mater., 2002, 14, 2649; (c) J. Lu, E. H. Shen, M. Yuan, Y. G. Li, E. B. Wang, C. W. Hu, L. Xu and J. Peng, Inorg. Chem., 2003, 42, 6956; (d) X. Y. Zhao, D. D. Liang, S. X. Liu, C. Y. Sun, R. G. Cao, C. Y. Gao and Y. H. Ren, Inorg. Chem., 2008, 47, 7133; (e) C. M. Liu, D. Q. Zhang, M. Xiong and D. B. Zhu, Chem. Commun., 2002, 1416; (f) L. Lisnard, A. Dolbecq, P. Mialane, J. Marrot, E. Codjovi and F. Sécheresse, Dalton Trans., 2005, 3919; (g) H. Jin, Y. F. Qi, E. B. Wang, Y. G. Li, X. L. Wang, C. Qin and S. Chang, Cryst. Growth Des., 2006, 6, 2693; (h) W. J. Wang, L. Xu, G. G. Gao, L. Liu and X. Z. Liu, CrystEngComm., 2009, 11, 2488; (i) A. X. Tian, J. Ying, J. Peng, J. Q. Sha, Z. M. Su, H. J. Pang, P. P. Zhang, Y. Chen, M. Zhu and Y. Shen, Cryst. Growth Des., 2010, 10, 1104; (j) J. Q. Sha, J. W. Sun, M. T. Li, C. Wang, G. M. Li, P. F. Yan and L. J. Sun, Dalton Trans., 2013, 42, 1667.
- (13) (a) B. X. Dong, J. Peng, C. J. Gomez-Garcia, S. Benmansour, H. Q. Jia and N. H. Hu, *Inorg. Chem.*, 2007, 46, 5933; (b) Y. P. Ren, X. J. Kong, X. Y. Hu, M. Sun

- and L. S. Long, *Inorg. Chem.*, 2006, **45**, 4016; (c) Y. P. Ren, X. J. Kong, L. S. Long, R. B. Huang and L. S. Zheng, *Cryst. Growth Des.*, 2006, **6**, 572.
- (14) (a) W. G. Klemperer, T. A. Marquart and O. M. Yaghi, *Angew. Chem., Int. Ed.*, 1992, 31, 49. (b) W. G. Klemperer, T. A. Marquart and O. M. Yaghi, *Angew. Chem. Int. Ed.*, 1992, 104, 51; (c) V. W. Day, W. G. Klemperer and O. M. Yaghi, *J. Am. Chem. Soc.*, 1989, 111, 5959; (d) G. K. Johnson and E. O. Schlemper, *J. Am. Chem. Soc.*, 1978, 100, 3645; (e) L. Chen, F. L. Jiang, Z. Z. Lin, Y. F. Zhou, C. Y. Yue and M. C. Hong, *J. Am. Chem. Soc.*, 2005, 127, 8588; (f) M. I. Khan and J. Zubieta, *Angew. Chem., Int. Ed.*, 1994, 33, 760.
- (15) Sheldrick, G. M. SADABS 2.05; University of Göttingen: Göttingen, Germany.
- (16) SHELXTL 6.10; Bruker Analytical Instrumentation: Madison, WI, 2000.
- (17) (a) C. J. Zhang, H. J. Pang, Q. Tang, H. Y. Wang and Y. G. Chen, New J. Chem., 2011, 35, 190; (b) C. J. Zhang, H. J. Pang, Q. Tang, H. Y. Wang and Y. G. Chen, Dalton Trans., 2010, 39, 7993.
- (18) H. T. Evans and M. T. Popev, *Inorg. Chem.*, 1984, **23**, 501.
- (19) I. D. Brown and D. Altermatt, Acta Crystallogr. Sect. B: Struct. Sci., 1985, 41, 244.
- (20) A. W. Addison and T. N. Rao, *J. Chem. Soc. Daltontrans.* 1984, 1349.
- (21) J. Q. Sha, J. Peng, Y. Zhang, H. J. Pang, A. X. Tian, P. P. Zhang and H. Liu, *Cryst Growth Des.*, 2009, **9**, 1708.
- (22) (a) L. Carlucci, G. Ciani, D. M. Proserpio and F. Porta, *Angew. Chem., Int. Ed.*, 2003, 42, 317; (b) X. S. Qu, L. Xu, G. G. Gao, F. Y. Li and Y. Y. Yang, *Inorg.*

- Chem., 2007, 46, 4775.
- (23) (a) Y. Q. Lan, S. L. Li, X. L. Wang, K. Z. Shao, D. Y. Du, H. Y. Zang and Z. M. Su, *Inorg. Chem.*, 2008, 47, 8179. (b) X. L. Wang, Q. Gao, A. X. Tian, H. L. Hu and G. C. Liu, *J. Solid. State. Chem.*, 2012, 187, 219.
- (24) (a) P. P. Zhang, J. Peng, H. J. Pang, Y. Chen, M. Zhu, D. D. Wang, M. G. Liu and Y. H. Wang, *Inorg. Chem. Commun.*, 2010, 13, 1414; (b) H. J. Pang, M. Yang, H. Y. Ma, L. Kang, B. Liu and S. B. Li, *J. Solid. State. Chem.*, 2013, 198, 440.
- (25) Q. G. Zhai, X. Y. Wu, S. M. Chen, Z. G. Zhao and C. Z. Lu, *Inorg. Chem.*, 2007, 46, 5046.
- (26) W. G. Klemperer and W. J. Shum, Am. Chem. Soc., 1976, 98, 8291.
- (27) (a) S. Horike, D. Tanaka, K. Nakagawa and S. Kitagawa, *Chem. Commun.*, 2007, 3395; (b) D. Tanaka, K. Nakagawa, M. Higuchi, S. Horike, Y. Kubota, T. C. Kobayashi, M. Takata and S. Kitagawa, *Angew. Chem. Int. Ed.*, 2008, 47, 3914.
- (28) (a) Y. Bai, G. Q. Zhang, D. B. Dang, P. T. Ma, H. Gao and J. Y. Niu, CrystEngComm., 2011, 13, 4181; (b) S. Igawa, M. Hashimoto, I. Kawata, M. Hoshino and M. Osawa, Inorg. Chem., 2012, 51, 5805.
- (29) Y. C. Qiu, Z. H. Liu, Y. H. Li, H. Deng, R. H. Zeng and M. Zeller, *Inorg. Chem.*, 2008, 47, 5122.
- (30) (a) X. He, J. Zhang, X. Y. Wu and C. Z. Lu, *Inorg. Chim. Acta.*, 2010, 363, 1727;
 (b) W. Li, H. P. Jia, Z. F. Ju and J. Zhang, *Cryst. Growth Des.*, 2006, 6, 2136; (c)
 Z. Su, J. Fan, M. Chen, T. A. Okamura and W. Y. Sun, *Cryst. Growth Des.*, 2011,

- **11**, 1159.
- (31) V. Ramamurthy, In Photochemistry in Organized and Constrained Media; Ramamurthy, V., Ed.; VCH Publishers: New York, 1991.
- (32) (a) H. Jin, Y. F. Qi, E. B. Wang, Y. G. Li, C. Qin, X. L Wang and S. Chang, Eur. J. Inorg. Chem., 2006, 4541; (b) C. Qin, X. L. Wang, Y. F. Qi, E. B. Wang, C. W. Hu and L. Xu, J. Solid State Chem., 2004, 177, 3263.
- (33) X. L. Wang, Q. Gao, A. X. Tian, H. L. Hu and G. C. Liu, J. Solid State Chem., 2012, 187, 219.
- (34) C. D. Zhang, S. X. Liu, C. Y. Sun, F. J. Ma and Z. M. Su, *Cryst. Growth Des.*, 2009, **9**, 3655.
- (35) (a) S. B. Li, W. Zhu, H. Y. Ma, H. J. Pang, H. Liu and T. T. Yu, RSC. Advances.,
 2013, 3, 9770. (b) A. X. Tian, J. Ying, J. Peng, J. Q. Sha, H. J. Pang, P. P. Zhang,
 Y. Chen, M. Zhu and Z. M. Su, Inorg. Chem., 2009, 48, 100.
- (36) (a) S. Y. Zhu, H. J. Li, W. X. Niu and G. B. Xu, *Biosensors and Bioelectronics*., 2009, **25**, 940; (b) B. X. Dong, J. Peng, A. X. Tian, J. Q. Sha, L. Li and H. S. Liu, *Electrochimica Acta.*, 2007, **52**, 3804.